



ELSEVIER

Ultramicroscopy 92 (2002) 67–76

ultramicroscopy

www.elsevier.com/locate/ultramic

Bias-induced forces in conducting atomic force microscopy and contact charging of organic monolayers

X.D. Cui^a, X. Zarate^b, J. Tomfohr^a, A. Primak^{b,c}, A.L. Moore^b, T.A. Moore^b,
D. Gust^b, G. Harris^c, O.F. Sankey^a, S.M. Lindsay^{a,*}

^a *Department of Physics and Astronomy, Arizona State University, Tempe, AZ 85287-1504, USA*

^b *Department of Chemistry and Biochemistry, Arizona State University, Tempe, AZ 85287-1504, USA*

^c *Motorola Inc., 2100 East Elliot Road, AZ34/EL 704, Tempe, AZ 85284, USA*

Received 16 July 2001; received in revised form 14 November 2001; accepted 20 November 2001

Abstract

Contact electrification, a surface property of bulk dielectric materials, has now been observed at the molecular scale using conducting atomic force microscopy (AFM). Conducting AFM measures the electrical properties of an organic film sandwiched between a conducting probe and a conducting substrate. This paper describes physical changes in the film caused by the application of a bias. Contact of the probe leads to direct mechanical stress and the applied electric field results in both Maxwell stresses and electrostriction. Additional forces arise from charge injection (contact charging). Electrostriction and contact charging act oppositely from the normal long-range Coulomb attraction and dominate when a charged tip touches an insulating film, causing the tip to deflect away from the film at high bias. A bias-induced repulsion observed in spin-coated PMMA films may be accounted for by either mechanism. In self-assembled monolayers, however, tunnel current signals show that the repulsion is dominated by contact charging. © 2002 Elsevier Science B.V. All rights reserved.

1. Introduction

The scanning tunneling microscope (STM) has been widely used in molecular electronics research [1–8] but it suffers from the drawback that the contact force is not controlled independently. Just how hard the STM tip ‘touches’ an organic monolayer is still a matter of debate [9]. Modified STMs have been designed to monitor [10] or regulate [11] this contact force. A simpler approach is to use a conducting atomic force microscope (AFM) in which a conventional

force-sensing cantilever is coated with a conducting layer so that electronic and mechanical properties may be measured simultaneously [12–15]. In these experiments, a probe of end-radius on the order of a few nanometers is pressed against the film with a force of a few nanoNewtons, resulting in GPa stresses in the film. These stresses, and their effect on the measured tunnel current, have been discussed at length elsewhere [13,16]. The question arises as to whether or not there are significant changes in contact force as the bias applied between a tip and a sample is varied, and, if there are such variations, the degree to which they may influence the electronic

*Corresponding author. Fax: +1-602-965-7954.

measurements. This is the subject of the present paper.

We have monitored the AFM deflection signal as the bias is varied while a conducting AFM contacts organic thin films, finding significant bias-dependent deflection. Intriguingly, this deflection signal is just the opposite of what might be expected for the Coulomb attraction between the tip and the underlying substrate. According to conventional theory, a non-piezoelectric elastomeric material, subject to an electric field, E , is strained (S_{zz}) in the field direction, z , according to

$$S_{zz} \cong -\frac{1}{2Y} \varepsilon \varepsilon_0 E^2 \left[2 - \frac{a_1}{\varepsilon} \right], \quad (1)$$

where Y is the Young's modulus of the film, ε its dielectric constant and a_1 describes the electrostrictive response of the material (from Krakovsky et al. [17] with the assumption that Poisson's ratio for the film is 0.5). The first term describes a compressional strain caused by Coulomb attraction between the opposite charges on the opposite surfaces of the film. The corresponding stress is known as the Maxwell stress. The second term has the opposite sign and describes an expansion of the film owing to electrostriction.

We have discovered an additional deflection signal that occurs *without* strains in the field direction, and propose that it arises from a Coulomb repulsion between injected charge and charge on the AFM probe. Contact charging (also known as contact electrification or triboelectricity) is the process whereby an insulating surface acquires a charge on contact with another insulator or a metal [18]. Its origin remains a mystery till today. The most studied case is the charging of an insulating surface upon contact with a metal. Scanning probe methods have permitted studies of this phenomenon, free from uncertainties associated with the geometry of macroscopic contacts [19–24]. These studies have led to the following conclusions: (1) The charging process is electronic as opposed to ionic. (2) A neutral metal tip can deposit both positive (holes) and negative (electrons) charges, so that the local charge density may be much higher

than the macroscopically measured surface charge. (3) A charged metal tip deposits charge in proportion to its charge, as controlled by the potential difference applied to connections that form a capacitor enclosing the dielectric film. (4) The deposited charge spreads over a region much larger than the size of the contact. A recent study concluded that atmospheric oxygen might play a role [25].

Prior scanning probe studies of contact charging have all used macroscopic polymer (or carbon [25]) films or spheres, the surface geometries of which are not well characterized on the atomic scale. Measurements were based on non-contact detection of previously injected surface charge. Gady et al. [22–24] measured the force on a charged tip as it was swept towards (or away from) a charged surface, including that of a polymer sphere charged by contact with a graphite surface throughout the duration of the measurement. Terris and co-workers [19–21,26,27] scanned a metalized AFM cantilever above a surface while applying an oscillating bias between the cantilever and an electrode below the surface. An image of the displacement signal from the cantilever at the driving frequency mapped fixed charge on the surface, while an image formed from the first harmonic of this signal mapped the polarizability of the surface (because of the quadratic dependence of this force on voltage). A similar approach, called scanning polarization force microscopy [28] was used to study contact charging of hard disk surfaces [25].

These scanning probe methods are sensitive to charges as small as a few electrons, but they require that the sample remains charged for an extended period after contact charging. AFM images taken after a polymer surface was contacted with a tip to show that the charge decays over time after the contact is removed [19]. In this work, a new method is demonstrated for detecting charge injection while the probe remains in contact with the film.

We will first describe electric force measurements both in contact and out of contact with a polymethylmethacrylate (PMMA) film, a material known to undergo contact electrification [20].

A bias-dependent repulsive deflection signal is observed in contact, but it could be accounted for either by electrostriction or by contact charging. A similar repulsive deflection is observed when the probe contacts alkanethiol monolayers. In this case, tunnel current measurements show that the film thickness does not change as bias is swept, and this implies that the repulsion is caused by contact electrification. The occurrence of contact electrification is verified by non-contact imaging. This new approach has been used to study a number of different monolayers. Contact electrification is observed in all the films studied with the exception of a highly conductive 4-aminothiophenol monolayer and an octanedithiol chemically bonded into the tip–substrate junction.

2. Experimental

Measurements were made using a PicoSPM conducting AFM (Molecular Imaging, Phoenix). The conducting force-sensing probe is connected to the virtual ground of a current-to-voltage converter with 1 V/nA sensitivity and a noise level of $0.011\text{ pA}/\sqrt{\text{Hz}}$. The sample is isolated from ground and connected to a programmable bias voltage. The microscope is equipped with a hermetically sealed sample chamber flushed with nitrogen or argon to reduce oxygen and water vapor contamination. The sample may also be submerged in a liquid using an integrated liquid cell. We used Pt-coated silicon cantilevers with a spring constant of 0.35 N/m (Molecular Imaging). Gold coated cantilevers were prepared by sputter-coating silicon cantilevers (0.35 N/m) with 5 nm of Cr followed by 50 nm of Au.

Samples were deposited onto Au(111) substrates formed by evaporation of 200 nm of Au onto freshly cleaved heated mica substrates in ultrahigh vacuum [29]. The substrates were reannealed with a hydrogen flame immediately prior to deposition of the sample.

Octanethiol, decanethiol, dodecanethiol, tetradecanethiol, 11-mercapto-1-undecanol, 4-aminothiophenol, and 1,8 octanedithiol were purchased from Aldrich and used without further purification. Docosanethiol was prepared from its

corresponding bromide (Aldrich) by reaction with thiourea and subsequent base hydrolysis of the adduct. Toluene and hexane (Aldrich) were freshly distilled before each experiment. The liquid cell was routinely cleaned as described elsewhere [13]. PMMA films were spin coated onto the gold substrates to a final thickness of 100 nm at the Center for Solid State Electronics Research at ASU. We examined both as-prepared and UV crosslinked PMMA films. For simplicity, all alkanethiols are referred to by the number of carbon atoms in the chain; $\text{HS}-(\text{CH}_2)_{11}-\text{CH}_3$ is called C12 alkanethiol, for example.

Monolayers of thiolated molecules were prepared from 1 mM solutions in either toluene or hexane. Freshly annealed Au substrates were submerged in these solutions for 12 h . The samples were copiously rinsed with freshly distilled solvent and then mounted in the AFM chamber under toluene or hexane, or dried under N_2 or Ar gas. A flow of inert gas was also maintained through the environmental chamber that encloses the liquid cell in all these experiments. Controlled humidification was achieved by mixing wet and dry argon. It was monitored with a hygrometer in the sample chamber. The partial pressures of O_2 and H_2O in the experimental chamber in dry conditions are not known, but they were presumably low. For example, current–voltage curves changed irreversibly within seconds of exposure of the sample to ambient air.

All measurements were made with the built-in software of the PicoSPM, with the exception of the non-contact charge imaging. This was carried out using a Stanford Research Systems SR830 lock-in amplifier with built-in signal source. Signals were supplied to the microscope, and read from it, using a breakout box (Molecular Imaging) and an oscillating tip bias of 50 mV amplitude at a frequency of 13 kHz . The synchronously detected deflection signal was fed into the auxiliary imaging channel of the PicoSPM controller. The experimental layout was as described by Terris et al. [20] except that the tip was scanned across the surface in non-contact mode simply by lifting it about 10 nm above the surface after determining the contact point directly.

3. Results and discussion

3.1. Electric force measurement on PMMA films

Fig. 1a shows the deflection of the cantilever probe as a function of the bias applied between the Pt layer on the probe and the gold film underlying the polymer film. The magnitude of the deflection was calibrated using a conventional force curve, an example of which is shown for zero bias in a dry nitrogen environment in Fig. 1b. This curve, and all similar curves were obtained by switching off the height servo when the instrument was sufficiently stable so that drift did not affect the reproducibility of the curves over the period (ca. 0.1 s) required for recording. Out of contact, the displacement, ΔZ , reflects the Coulomb attraction, and is well fitted by a parabolic function of voltage:

$$\Delta Z = \frac{F}{k} = \frac{1}{2k} \frac{\partial C}{\partial Z} (V + V_a)^2. \quad (2)$$

Here Z is an effective height of the tip from the surface (it is related to physical height via the charge distribution on the tip), k is the cantilever force constant, C is the tip–substrate capacitance

and V_a is the contact potential difference [30,31]. $\partial C/\partial Z$ is <0 so that the force is attractive. Fits to these data yield values for $\partial C/\partial Z$ that agree with a simple capacitor model [20].

When the tip just contacts the surface, a parabolic deflection signal is also observed, but *inverted* with respect to the non-contact curves and much reduced in magnitude (bottom curve in Fig. 1a). The contact point is determined in the usual way by plotting the deflection of the cantilever as a function of its vertical displacement (Fig. 1b) and the inversion of the force vs. voltage curve occurs precisely at the contact point. Normal behavior is restored as soon as the tip is pulled out of contact.

Electrostriction is one possible explanation for this repulsive displacement in contact (we discuss a possible artifact owing to cantilever deformation below). From Eq. (1):

$$\Delta Z = \frac{M}{Z} (V - V_r)^2, \quad (3)$$

where V_r is the contact potential difference (the change in notation allowing for the possibility that this quantity changes on contact) and M is the electrostrictive constant, $-(1/2Y)\epsilon\epsilon_0[2 - a_1/\epsilon]$.

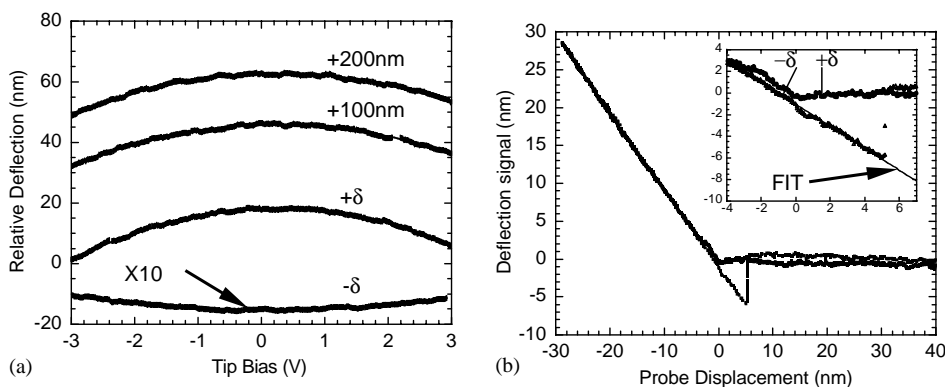


Fig. 1. (a) Force measurements on a cross-linked PMMA film under hexane, showing cantilever deflection signal vs. cantilever bias for tip positions: (1) 200 nm from the surface, (2) 100 nm from the surface, (3) just above the surface ($+\delta$ in the approach curve shown in (b)) and (4) just in contact ($-\delta$) with the surface. Data are for a cross-linked PMMA film under hexane and all curves have been displaced arbitrarily in the vertical direction for clarity. Almost identical data (not shown) were obtained for dry films in nitrogen gas. The signal in contact is shown magnified $10\times$. Out of contact, the curves are excellent fits to the parabolic function given in Eq. (2) with $V_a = 0.25 \pm 0.03$ V (lines are hidden by data points). In contact, the data are also well-fitted by Eq. (3), with $V_r = 0.12 \pm 0.09$ V. (b) Force curve taken from a similar film under dry nitrogen gas. The negative force on retraction reflects substantial adhesion between the probe and the film, indicating that the tip remains in contact with the film during the repulsive deflection observed after contact. The inset is an expanded view of the force curve in the vicinity of contact. The retraction curve has been fitted to a straight line (FIT above), showing that the film does not undergo substantial deformation on this length scale.

Typical values for polymers are of the order of $10^{-17} \text{ m}^2 \text{ V}^{-2}$ [32], so for this 100 nm film, a 3 V bias would result in about 1 nm of displacement, similar to the measured displacement (the contact curve is magnified $10 \times$ in Fig. 1a).

PMMA is also known to charge on contact with a Pt tip [20]. The injected charge varies with applied bias and spreads over an area substantially greater than that of the contact. This injected charge, interacting with the charge on the tip, will also give rise to a repulsive interaction. It is not possible to distinguish such an effect from the

electrostriction, which appears to give an adequate account of the repulsive deflection in this case.

3.2. Electric force measurements on organic monolayers

Similar bias-dependent cantilever deflection signals were observed for various self-assembled organic monolayers. Examples shown in Fig. 2 are C10 alkanethiol in dry nitrogen (a) the same sample submerged in hexane (b) and a C11-OH monolayer submerged in toluene (c). All show the

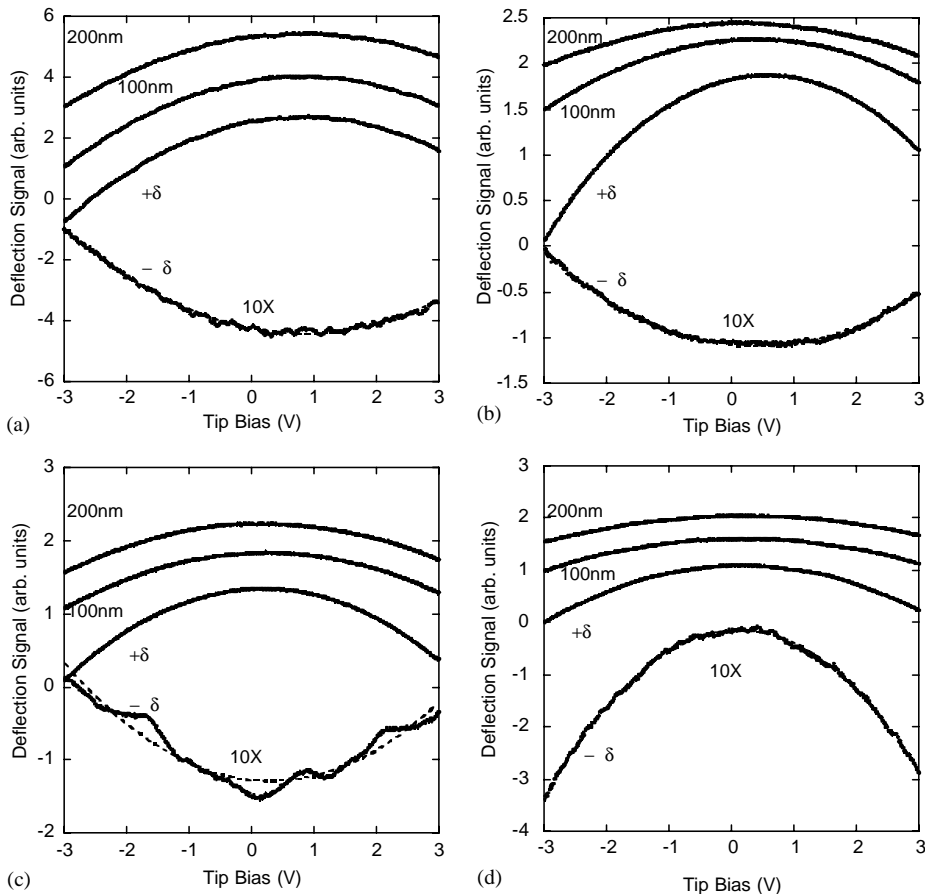


Fig. 2. Raw deflection signal (in volts) as a function of tip bias for: (a) C10 alkanethiol with a Pt tip in a nitrogen atmosphere, (b) C10 alkanethiol with an Au tip in hexane, (c) C11-OH alkanethiol with a Pt tip in toluene and (d) 4-aminothiophenol with a Pt tip in toluene for heights of 200, 100 nm, just above the sample ($+\delta$) and just in contact ($-\delta$). The signal in contact is shown multiplied $10 \times$ and all curves have been displaced arbitrarily in the vertical direction for clarity. Dashed lines are fits to the parabolas, Eqs. (2) and (3), and they are visibly distinct from the data points only in (c). Deflection signals can be converted to a repulsive force in nanoNewtons by multiplying by 11.7 (or 1.17 for data plotted $10 \times$).

transition from an attractive interaction out of contact to a repulsive interaction as soon as the tip contacts the monolayer. We have also observed these effects in other samples (summarized below). An exception is the highly conductive 4-aminothiophenol monolayer for which data are shown in Fig. 2d. Here, the deflection signal in contact indicates an attractive interaction.

Does the similarity between these data and those just presented for PMMA films imply that electrostriction plays a role? In the case of these thin films, tunnel current can be recorded at the same time as deflection. The tunnel current data give no indication of significant changes in the dimensions of the samples as bias is changed. Many examples of current–voltage curves for these films have been given elsewhere [16] and they show a continuous increase of current with voltage in line with the predictions of tunneling theory. A motion of several nanometers away from the film would surely cause the tip to leave the surface altogether. A further example is given in Fig. 3 where the current through an octanethiol monolayer is shown for a voltage sweep with the AFM force servo off and, subsequently with the force servo on. The force servo adjusts the height of the tip to compensate for the deflection that occurs as

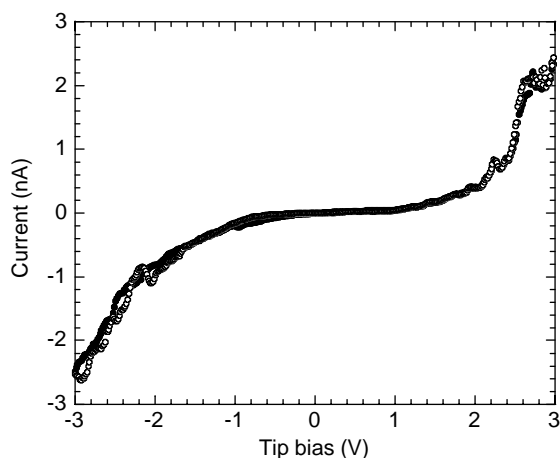


Fig. 3. Current–voltage curves taken from an octanethiol monolayer with the force servo off (open circles) and, subsequently with the force servo on (filled circles). The smooth rise of current with voltage and the small effect of turning the servo on preclude the possibility of significant vertical displacement of the tip with bias.

the bias is swept, in this case, moving the sample towards the tip by about 3 nm at the highest bias. The two curves are almost identical, implying that the vertical distance between the tip and substrate could not have changed. The 4-aminothiophenol case is even more extreme. Here (Fig. 2d), the deflection *towards* the surface would be nearly 10 nm, many times the dimension of the molecule! *Clearly these deflection signals must be generated while the apex of the tip remains at a constant vertical height above the substrate.*

3.3. Cantilever mechanics with the apex of the tip fixed

Deflection of the cantilever through a vertical displacement of the tip ΔZ is detected as an angular deflection $\delta\theta_1 = \Delta Z/L$ where L is the length of the cantilever (Fig. 4a). When the tip rests on a hard surface and is moved vertically so as to cause deflection, this angular motion appears as a consequence of a torque on the tip (Fig. 4b). When the tip is raised (relative to the cantilever base) a distance ΔZ by being pushed against a surface, its vertical axis must also rotate by an angle $\delta\theta_1 = \Delta Z/L$. The restoring force, F_S , of the cantilever spring is applied to one side of the tip only and F_S and the equal and opposite normal force, N , constitute a couple acting over some distance λ (λ is a function of cantilever geometry). Consequently, an equivalent calculation of the cantilever bending is obtained by equating the torque on the cantilever to the torsional restoring force caused by the cantilever bending. Referring to Fig. 4b, this yields $F_S\lambda = \tau\delta\theta_1$, where τ is the torsional force constant of the cantilever. In the case of a vertical displacement, $F_S = k\Delta Z$, leading to $\tau = kL\lambda$, where k is the cantilever spring constant, so the description is entirely equivalent to equating the bending signal to a vertical displacement and calculating a force from this displacement and the cantilever spring constant.

In the case where a significant additional interaction, F_R exists between the surface and the tip, $N \neq -F_S$. This extra force, F_R , will result in an extra torque $F_R\lambda$ with a corresponding rotation $\delta\theta_2 = F_R\lambda/\tau + \delta\theta_1 = F_R/kL + \Delta Z/L$ (Fig. 4c). Note that, because the tip remains in contact with

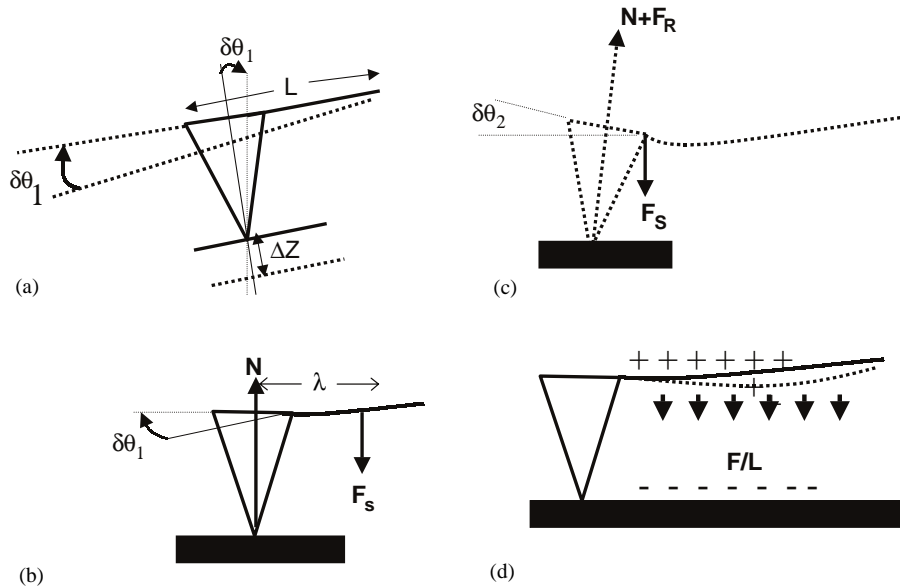


Fig. 4. Showing tip mechanics in contact. In order to displace the end of the cantilever by an amount ΔZ , a tip in contact with a hard surface rotates by $\delta\theta_1$ radians (equal to $\Delta Z/L$) shown here in (a). If all the deflection is generated by movement of the surface, the normal force, N , is equal in magnitude and opposite in direction to the force generated by the cantilever spring, F_S , resulting in a torque, $F_S\lambda$, that rotates the end of the cantilever and tip. The balance of torques is shown in (b). Changes in the normal force owing to other interfacial interactions change the net value of this torque, causing an additional bending signal with *no* vertical motion of the end of the tip as shown in (c). (d) Showing how a Coulomb attraction between the cantilever and the substrate can translate into an apparent ‘repulsive’ deflection signal when the tip contacts the surface. This effect is very small as described in the text.

a hard surface as this force is applied, no vertical motion will occur unless this additional force is large enough to push the tip out of contact with the surface. This result is equivalent to the effect of an additional ‘displacement’, $\Delta Z_2 = \delta\theta_2 L = F_R/k$. (Some additional buckling of the cantilever will occur if the tip is not free to slide on the surface, but the effect is generally small.)

It is important to consider possible spurious responses. One such artifact is illustrated in Fig. 4c. This shows how a Coulomb *attraction* between the cantilever body and the substrate can result in an apparent *repulsion* as the cantilever is pulled into the surface, bending against the fixed tip. If the cantilever has area A and is located a distance h above the surface, this attractive force is $\epsilon_0 AV^2/h^2$, where we have assumed an intervening relative dielectric constant of unity. In our case, $h \approx 10 \mu\text{m}$, $A \approx 27 \times 270 \mu\text{m}$ leading to a total Coulomb force of about 5 nN at 3 V. This will produce a maximum deflection of the center of the cantilever, $y = \frac{1}{364} fL^3/EI$ [33] where F is the total

distributed force, E the Young’s modulus of silicon ($1.8 \times 10^{11} \text{ N/m}^2$) and I the bending moment. For a cantilever width of $27 \mu\text{m}$ and a thickness $3 \mu\text{m}$, $I = 1.2 \times 10^{-22} \text{ m}^4$ so that $y = 1.5 \times 10^{-11} \text{ m}$, giving a bending angle of 10^{-7} rad ($2y/L$). In the experiments reported here, the cantilever deflection signals correspond to much larger angles (of the order of 10^{-5} rad) so this spurious response is not significant. Thus we conclude that ‘repulsive’ angular motion of the cantilever can be caused without vertical displacement of the tip by bias-induced repulsive forces such as those caused by charge injection.

3.4. Independent confirmation of contact charging in alkanethiol monolayers

Contact electrification has not previously been demonstrated on self-assembled molecular monolayers, so the imaging method of Terris et al. [20] was applied to alkanethiol monolayers in order to detect charging of this sample with a well-tried

technique. This requires that the tip, charged by application of a large potential, be contacted against the surface transiently, then withdrawn and subsequently used to image the region of the contact. The image is formed using the output of a lock-in amplifier driven with the AFM deflection signal, with the bias modulation as a reference. This method is limited by the lifetime of the stored charge, which, even on the thicker molecular layers charged at tip potentials of several volts, lasted for only a few minutes at most. An example is shown in Fig. 5, where a C12 alkanethiol layer was charged by contact with a Pt tip biased at +5 V. Intensities of the charge images were highly variable, consistent with the observed rapid decay of the stored charge. We found that negative charge could be injected with equal facility. The method is difficult to characterize, however, because the lifetime of the stored charge is short and highly variable.

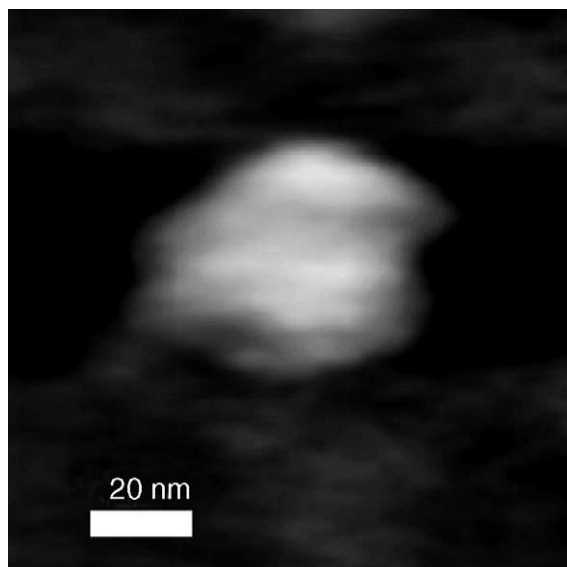


Fig. 5. Non-contact image of surface charge on a C12 alkanethiol monolayer submerged in toluene. A Pt tip was biased to +5 V and briefly contacted against the film at low contact force (<1 nN). The tip was withdrawn about 10 nm and the region scanned to yield this image of the deflection signal component at the voltage modulation frequency, a small modulation being applied to a tip at a mean bias of 0 V. The total scan time was about 80 s. The charge was completely dissipated on the next and subsequent scans.

3.5. Characterization of the bias induced forces for various organic monolayers and films

Data for a number of samples in different conditions were fitted using Eq. (2) in the non-contact regime. In the contact regime, we used a generalization of Eq. (3)

$$F_r = K_r(V - V_r)^2, \quad (4)$$

where K_r is a parameter describing the strength of the voltage induced repulsion. Values for this parameter (in nN/V²) and the contact potentials, V_a and V_r are listed for various samples under toluene in Table 1, and for a variety of environments in Table 2.

The contact potential difference reflects dipole moments in the layer between the electrodes, being quantitatively equal to the dipole moment normal to the surface, μ_{\perp} , per unit area [30]:

$$V_a = \frac{\mu_{\perp}}{\epsilon_0 A}. \quad (5)$$

A value for μ_{\perp} is obtained from the normal component of the vector sum of all the dipole moments in the gap. It includes any dipole arising from contamination of the tip, so that only differences between samples measured with similar tips are meaningful. We note that the contact potential of the hydroxy-terminated monolayers is reduced by about 0.3 V relative to the methyl-terminated monolayers, consistent with the results of earlier work [30,31].

The strength of the contact-charge induced interaction is quite similar for all the samples and media studied with the exception of an octanedithiol monolayer contacted by a gold tip and the 4-aminothiophenol monolayer. The latter sample was highly conductive, passing three to four orders of magnitude more current at a given bias than the alkanethiol monolayers, and therefore, possibly incapable of storing charge. The octanedithiol connected to the gold tip was much more conductive than the alkanethiols but much less so than the 4-aminothiophenol monolayer. Interestingly, this film showed no measurable deflection, suggesting that charge injection into the traps responsible for contact charging is inhibited when the metal is chemically bonded to

the molecular monolayer. The Maxwell stress is not significant either, perhaps because of the greater thickness of this sample compared to 4-aminothiophenol (see Eq. (1)).

Within the group of compounds that manifest contact charging, neither the alkane chain length nor the end group appears to have a significant effect (Table 1). The effect is somewhat weaker in a hexane environment and under argon gas (Table 2). Following van den Oetelaar et al. [25], we checked the effect of humidifying the sample chamber in the presence of argon for a C10 alkanethiol monolayer. K_r fell by about 20% between 10% RH and 60% RH to a value half that measured under freshly distilled toluene. It is therefore possible that some of the environmental differences shown in Table 1 are a consequence of adventitious water contamination. We saw no effect of excluding atmospheric oxygen to the extent that we were able to control it.

4. Conclusions

We have demonstrated that electrically induced forces in samples subject to conducting AFM can be quite different from the long-range Coulomb attraction experienced by a free, biased conducting cantilever. With the exception of a highly conductive monolayer (4-aminothiophenol) and an octanedithiol monolayer chemically bonded to a gold tip, the films and monolayers examined here repel the tip as bias is increased with the tip in contact with the film. In the case of alkanethiol monolayers whose thickness can be monitored by tunneling, the effect occurs without vertical displacement of the tip. Thus, the repulsion cannot be accounted for by electrostriction of the films. We have shown how a repulsive force on the tip generates a torque that gives rise to a deflection signal equivalent to that obtained by moving the tip away from the surface, even though the apex of the tip remains fixed on the surface. One explanation for this effect is contact charging of the monolayers, and non-contact imaging of charge deposited by a prior contact shows that alkanethiol monolayers can indeed be charged this way. Measurements made on different samples in

different conditions do little to help build an explanation of the contact charging, save that we confirm the dissipative effect of water [25].

It is notable that the rather significant voltage induced deflection signals appear to occur in such a way as to minimize distortion of the current–voltage data collected by conducting AFM. One way to test for this is to collect data with and without the constant force servo enabled during the voltage scan. Both Maxwell stress and contact charging were absent in the sample chemically bonded into the tip–sample–substrate junction and this may prove a more reliable approach to the measurement of the electrical properties of organic monolayers.

Acknowledgements

We thank Mike Kozicki of the Center for Solid State Electronics Research for arranging preparation of the PMMA films. Jack Houston of Sandia labs suggested experiments in dry gas. John Mamin of IBM Almeden explained aspects of the charge imaging technique. Support was received from the NSF(DBI-951-3233, DMR-9632635 and CHE 0078835).

References

- [1] Z.J. Donhauser, B.A. Mantooth, K.F. Kelly, L.A. Bumm, J.D. Monnell, J.J. Stapleton, D.W. Price, A.M. Rawlett, D.L. Allara, J.M. Tour, P.S. Weiss, *Science* 292 (2001) 2303.
- [2] W. Han, E.N. Durantini, T.A. Moore, A.L. Moore, D. Gust, P. Rez, G. Leatherman, G.R. Seely, N. Tao, S.M. Lindsay, *J. Phys. Chem.* 101 (1997) 10719.
- [3] M.P. Samata, W. Tian, S. Datta, J.I. Henderson, C.P. Kubiak, *Phys. Rev. B* 53 (1996) 7626.
- [4] S. Datta, W. Tian, S. Hong, R. Reifengerger, J.I. Henderson, C.P. Kubiak, *Phys. Rev. Lett.* 79 (1997) 2530.
- [5] W. Tian, S. Datta, S. Hong, R. Reifengerger, J.I. Henderson, C.P. Kubiak, *J. Chem. Phys.* 109 (1998) 2874.
- [6] N. Tao, *Phys. Rev. Lett.* 76 (1996) 4066.
- [7] C. Joachim, J.K. Gimzewski, *Europhys. Lett.* 30 (1995) 409.
- [8] X. Lu, K.W. Hipps, *J. Phys. Chem.* 101 (1997) 5391.
- [9] K.A. Son, H.I. Kim, J.E. Houston, *Phys. Rev. Lett.* 86 (2001) 5357.

- [10] U. Durig, O. Zuger, B. Michel, L. Haussling, H. Ringsdorf, *Phys. Rev. B* 48 (1993) 1711.
- [11] F.R.F. Fan, J. Yang, S. Dirk, D.W. Proce, D. Kosynkin, J.M. Tour, A.J. Bard, *J. Am. Chem. Soc.* 123 (2001) 2452.
- [12] S.J. O'Shea, R.M. Atta, M.E. Welland, *Rev. Sci. Instrum.* 66 (1995) 2508.
- [13] G. Leatherman, E.N. Durantini, D. Gust, T.A. Moore, A.L. Moore, S. Stone, Z. Zhou, P. Rez, Y.Z. Li, S.M. Lindsay, *J. Phys. Chem. B* 103 (1999) 4006.
- [14] D.J. Wold, C.D. Frisbie, *J. Am. Chem. Soc.* 122 (2000) 2970.
- [15] D.J. Wold, C.D. Frisbie, *J. Am. Chem. Soc.* 123 (2001) 5549.
- [16] X.D. Cui, X. Zarate, J. Tomfohr, A. Primak, A.L. Moore, T.A. Moore, D. Gust, G. Harris, O.F. Sankey, S.M. Lindsay, *Nanotechnology*, 13 (2002) available on the web at <http://www.iop.org/EJ>.
- [17] I. Krakovsky, T. Romijn, A. Posthuma de Boer, *J. Appl. Phys.* 85 (1999) 628.
- [18] J. Lowell, A.C. Rose-Innes, *Adv. Phys.* 29 (1980) 947.
- [19] J.E. Stern, B.D. Terris, H.J. Mamin, D. Rugar, *Appl. Phys. Lett.* 53 (1988) 2717.
- [20] B.D. Terris, J.E. Sterns, D. Rugar, H.J. Mamin, *Phys. Rev. Lett.* 63 (1989) 2669.
- [21] B.D. Terris, J.E. Stern, D. Rugar, H.J. Mamin, *J. Vac. Sci. Technol. A* 8 (1990) 374.
- [22] B. Gady, R. Reifenberger, D.S. Rimai, L.P. DeMejo, *Phys. Rev. B* 53 (1996) 8065.
- [23] B. Gady, R. Riefenberger, D.S. Rimai, *J. Appl. Phys.* 84 (1998) 319.
- [24] B. Gady, R. Reifenberger, D.S. Rimai, L.P. DeMejo, *Langmuir* 13 (1997) 2533.
- [25] R.J.A. van den Oetelaar, L. Xu, D.F. Ogletree, H. Tang, J. Gui, *J. Appl. Phys.* 89 (2001) 3993.
- [26] F. Saurenbach, D. Wollmann, B.D. Terris, A.F. Diaz, *Langmuir* 8 (1992) 1199.
- [27] D. Rugar, H.J. Mamin, R. Erlandsson, J.E. Stern, B.D. Terris, *Rev. Sci. Instrum.* 59 (1988) 2337.
- [28] J. Hu, X.D. Xiao, M. Salmeron, *Appl. Phys. Letts.* 67 (1995) 476.
- [29] J.A. DeRose, T. Thundat, L.A. Nagahara, S.M. Lindsay, *Surf. Sci.* 256 (1991) 102.
- [30] R.C. Thomas, P. Tangyuyong, J.E. Houston, T.A. Michalske, R.M. Crooks, *J. Phys. Chem.* 98 (1994) 4493.
- [31] H. Takano, S.S. Wong, J.A. Harnisch, M.D. Porter, *Langmuir* 16 (2000) 5231.
- [32] A. Mujezinovic, *Electrostriction of silicone polymers*, M.S. Thesis, 1999, Arizona State University, Tempe, p. 62.
- [33] R.D. Cullum (Ed.), *Handbook of Engineering Design*, Butterworths, Boston, 1988.